

Effect of Cr, Mo and W on the Microstructure of Al Hot Dipped Carbon Steels

Trinh Van Trung¹, Min Jung Kim², Soon Yong Park², Poonam Yadav²,
Muhammad Ali Abro², and Dong Bok Lee^{2*}

¹School of Materials Science and Engineering, Hanoi University of Science and Technology, 1 Dai Co Viet Road, Hanoi, Vietnam

²School of Advanced Materials Science and Engineering, Sungkyunkwan University, Seobu-ro 2066, Suwon 440-746, Korea

(Received February 14, 2014; Revised February 21, 2014; Accepted February 24, 2014)

A low carbon steel, Fe-2.25%Cr steel (ASTM T22), and Fe-2.25%Cr-1.6%W steel (ASTM T23) were aluminized by hot dipping into molten Al baths. After hot-dipping, a thin Al-rich topcoat and a thick alloy layer formed on the surface. The topcoat consisted primarily of a thin Al layer that contained a small amount of Fe, whereas the alloy layer consisted of Al-Fe intermetallics such as Al₅Fe₂ and AlFe. Cr, Mo, and W in T22 and T23 steels reduced the thickness of the topcoat and the alloy layer, and flattened the reaction front of the aluminized layer, when compared to the low carbon steel.

Keywords : hot-dip aluminizing, low carbon steel, T22, T23

1. Introduction

Aluminizing by hot dipping steels in molten aluminum baths is an effective, economical method to form diffusion coatings to improve the oxidation and corrosion resistance of steels.¹⁾ The reaction between Al(l) and Fe(s) generally results in the formation of the Al-rich topcoat and the underlying Fe-Al alloy layer at the steel surface. The thickness, structure, and morphology of aluminized layers vary depending on the bath composition, dipping time, temperature, fluxing, substrate composition and surface roughness.²⁻¹³⁾ This led to diverse metallurgical reports about characteristics of the aluminized layers formed on carbon steels²⁻⁹⁾ and Cr-Mo steels.^{10,11)} An understanding about the microstructural changes of hot-dip aluminized steels as a function of the process parameters is therefore important. In order to investigate the effect of Cr and W on the microstructure of Al-hot dipped steels, a low carbon steel, an Fe-2.25%Cr steel (ASTM T22), and an Fe-2.25%Cr-1.6%W steel (ASTM T23) were aluminized by hot dipping into Al(l) baths and their microstructure was examined in this study.

2. Experimental

A low carbon ferritic steel (Fe-0.04C-0.15Mn in wt.%), a T22 ferritic steel (Fe-0.12C-2.25Cr-1.0Mo-0.45Mn in wt.%), and a T23 ferritic steel (Fe-0.06C-2.25Cr-1.6W-1.0Mo-0.45Mn in wt.%) with a size of 30x10x3 mm³ were cleaned ultrasoni-

cally in alcohol, immersed in 10 vol.% HCl solution to remove surface oxides, and subjected to the liquid flux treatment with 20 vol.% KCl+AlF₃ (in 4:1 weight ratio) solution in water. After drying, those samples were immersed for 10 min in a pure Al molten bath at 800 °C, on top of which a solid flux (KCl+NaCl+AlF₃ in 2:2:1 weight ratio) was spread to protect the molten baths from oxidation. The hot dipped specimens were pulled out at the speed of 20 cmmin⁻¹, cooled to room temperature in air, and further cleaned using 5 vol.% HNO₃ solution to remove any flux adhered on the aluminized surface. For microstructural analyses, they were cut into small coupons, mounted in the epoxy, ground, polished, and examined using a scanning electron microscope (SEM) equipped with an energy-dispersive spectroscope (EDS), and an X-ray diffractometer (XRD operated at 40 kV and 300 mA) with Cu-K α radiation.

3. Results and discussion

Fig. 1 shows SEM/EDS/XRD results of the low carbon steel. The aluminized surface was featureless, and smooth (Fig. 1(a)). The SEM image and the corresponding EDS line profiles shown in Figs. 1(b) and (c), respectively, indicate a thin Al topcoat (~25 μ m-thick), a thick alloy layer that consisted of Al-Fe intermetallics (~150 μ m-thick), and the Al-free steel substrate. The EDS spectra shown in Fig. 1(d) indicate that the top coat (spot ① indicated in Fig. 1(b)) and the alloy layer (spot ② indicated in Fig. 1(b)) were mainly composed of 99.7%Al-0.3%Fe and 73.7% Al-26.3%Fe, respectively. The XRD pattern shown in Fig.

* Corresponding author : dlee@skku.ac.kr

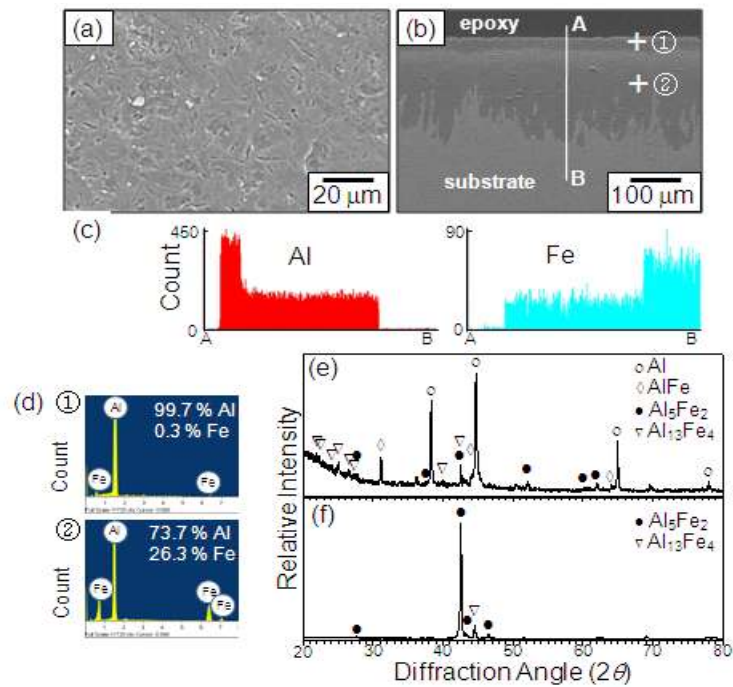


Fig. 1. Al hot dipped low carbon steel. (a) SEM top view, (b) cross-sectional SEM image, (c) EDS line profiles of Al and Fe along A-B, (d) EDS spectra of the spot ① and ②, (e) XRD pattern before grinding the surface, (f) XRD pattern after grinding off the outer coating layer.

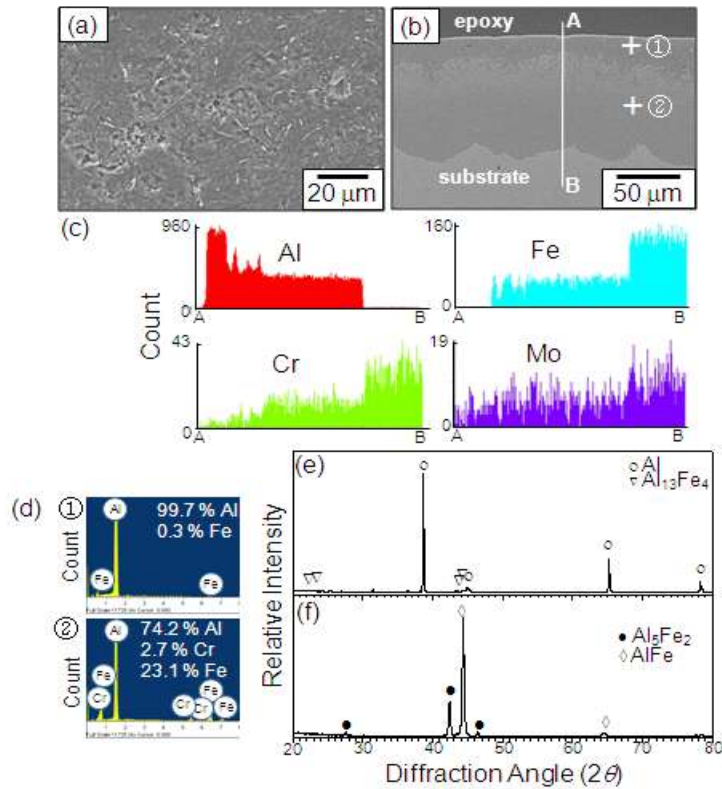


Fig. 2. Al hot dipped T22 steel. (a) SEM top view, (b) cross-sectional SEM image, (c) EDS line profiles of Al, Fe, Cr, and Mo along A-B, (d) EDS spectra of the spot ① and ②, (e) XRD pattern before grinding the surface, (f) XRD pattern after grinding off the outer coating layer.

1(e) indicates that the top coat consisted of Al as the major phase, and AlFe, Al₅Fe₂, Al₁₃Fe₄ (sometimes referred as Al₃Fe) as the minor phases. The XRD pattern shown in Fig. 1(f) indicates that the alloy layer consisted primarily of Al₅Fe₂, together with a small amount of Al₁₃Fe₄. The minor alloying element such as Mn in the low carbon steel was not able to identify in Figs. 1(c)-(f) due to its low concentration.

Fig. 2 shows SEM/EDS/XRD results of the T22 steel. A featureless, smooth aluminized surface was seen in Fig. 2(a). Figs. 2(b) and (c) indicate a thin Al topcoat (~20 μm-thick), a thick alloy layer that consisted of Al-Fe intermetallics (~80 μm-thick), and the Al-free steel substrate. Cr and Mo incorporated in the alloy layer more than the Al topcoat. Their amount was small, and their distribution would depend on their solubility and diffusivity in the aluminized layers. The EDS spectra shown in Fig. 2(d) indicate that the top coat (spot ① indicated in Fig. 2(b)) and the alloy layer (spot ② indicated in Fig. 2(b)) was mainly composed of 99.7%Al-0.3%Fe and 74.2%Al-23.1

%Fe-2.7%Cr, respectively. Fig. 2(e) indicates that the top coat consisted primarily of Al with a bit of Al₁₃Fe₄. Fig. 2(f) indicates that the alloy layer consisted of AlFe and Al₅Fe₂. The addition of Cr and Mo accelerated the formation of AlFe in the alloy layer.

Fig. 3 shows SEM/EDS/XRD results of the T23 steel. The aluminized surface shown in Fig. 3(a) was similar with those shown in Figs. 1(a) and 2(a). Figs. 3(b) and (c) indicate a thin Al topcoat (~20 μm-thick), a thick alloy layer that consisted of Al-Fe intermetallics (~50 μm-thick), and the Al-free steel substrate. In Fig. 3(c), Cr and W were present in the aluminized layer to a small amount. As shown in Figs. 3(b) and (d), the Al topcoat (spot ①) and the alloy layer (spot ②) consisted primarily of 99.4% Al-0.6%Fe and 77.8%Al-21.7%Fe-0.5%Cr, respectively. Tungsten detected in Fig. 3(c) could not be identified in Fig. 3(d), owing to its small amount. As shown in Figs. 3(e) and (f), the XRD technique could not detect any (Cr, W, Mo, Mn)-related compounds, which was attributed to their small amount or dissolution in the

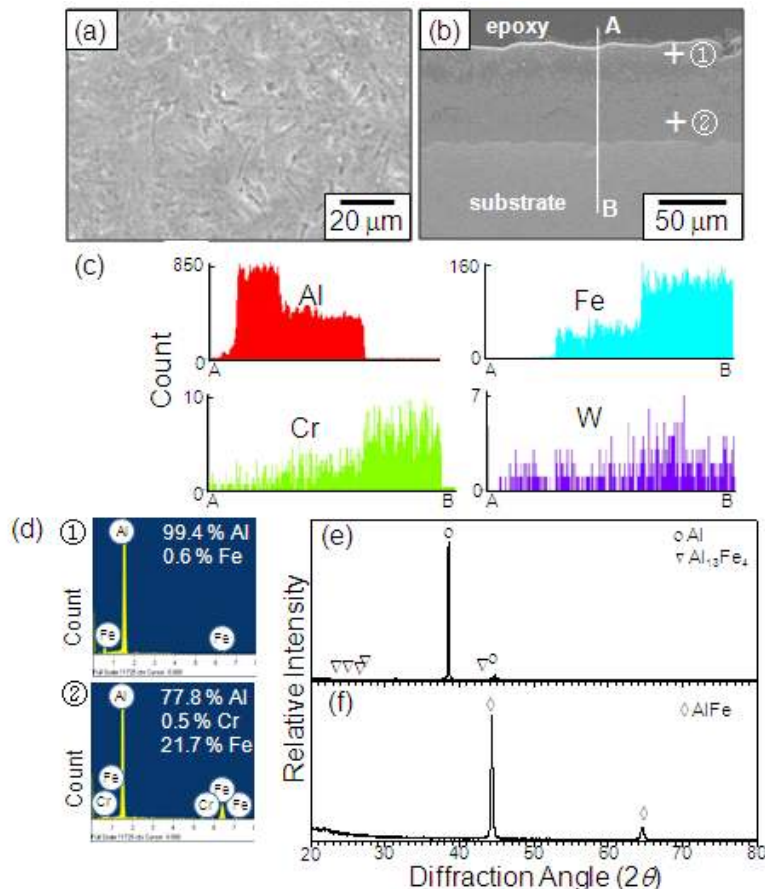


Fig. 3. Al hot dipped T23 steel. (a) SEM top view, (b) cross-sectional SEM image, (c) EDS line profiles of Al, Fe, Cr, and W along A-B, (d) EDS spectra of the spot ① and ②, (e) XRD pattern before grinding the surface, (f) XRD pattern after grinding off the outer coating layer.

Al-Fe intermetallic coating. The topcoat consisted of Al, together with a bit of Al_3Fe_4 (Fig. 3(e)). The alloy layer consisted mainly of AlFe (Fig. 3(f)). Not only Cr and Mo but also W was found to accelerate the formation of AlFe in the alloy layer. It is noted that AlFe can exist in the range of 23.3-55 at.%Al, according to the equilibrium Al-Fe phase diagram.

For all the samples, no cracks or voids were found in the aluminized coating, indicating a sound coating was achieved (Figs. 1(b), 2(b) and 3(b)). Depending on substrate materials and hot dipping conditions, alloy layers that consisted primarily of Al_5Fe_2 ,^{4-7,12,13} $\text{Al}_3\text{Fe}+\text{Al}_5\text{Fe}_2$,^{3,8,9,11} $\text{Al}_3\text{Fe}+\text{Al}_3\text{Fe}+\text{Al}_5\text{Fe}_2$,² and $\text{Al}_3\text{Fe}+\text{Al}_2\text{Fe}+\text{Al}_5\text{Fe}_2$ ¹⁰ were reported to form underneath the Al topcoat. The primary phase was usually reported to be Al_5Fe_2 in the case of carbon steels,⁷ as was also shown in Fig. 1(f). Lee et al.¹³ proposed that, based upon the thermodynamic consideration, Al_3Fe forms first at the Al(l)/Fe(s) interface, and reacts with Fe(s) to become Al_5Fe_2 , which grows inward. The formation of the tongue-like morphology shown in Figs. 1(b), 2(b), and 3(b) was attributed to the inward diffusion of Al from the molten bath through Al_5Fe_2 in the alloy layer to the Al_5Fe_2 /steel reaction front,⁷ or the outward diffusion of Fe from the substrate through the Al_5Fe_2 /steel reaction front into the Al_5Fe_2 phase,⁸ or the combination of these two diffusion processes.⁵ Such an explanation is based on the fact that diffusion occurs fast in orthorhombic Al_5Fe_2 with 30% of voids along the c-axis. Another possible explanation for the tongue-like morphology may be the atomic size mismatch between Al (atomic radius= 0.143 nm) and Fe (atomic radius= 0.126 nm).³

As shown in Figs. 1(d), 2(d), and 3(d), a small amount of Fe dissolved in the topcoat.¹¹ As shown in Figs. 2(c)-(d), and 3(c)-(d), a small amount of Cr, Mo, and W dissolved in the alloy layer.¹⁰ In this study, the interface between the alloy layer and the steel substrate became smooth, the thickness of the aluminized coating decreased as listed in Table 1, the interface between the alloy layer and the matrix became flattened, the formation of Al_5Fe_2 suppressed, and the formation of AlFe accelerated, with the addition of Cr and W. This may be originated from the fact that Cr and W occupy the vacant sites in Al_5Fe_2 to retard the diffusion along Al_5Fe_2 that has a high vacancy concentration in the c-axis.³ Since the growth rate of AlFe was slower than that of Al_5Fe_2 , the tongue-like morphology tends to disappear, and the aluminized coating becomes thinner with the addition of Cr, Mo, and W. It was previously reported that the adding of Si,^{2,3} W, Mo, and Nb¹² to the Al-melt has beneficially decreased the thickness of the alloy layer, and flattened the alloy lay

Table 1. Average thickness of the top coat and the alloy layer

	top coat (μm)	alloy layer (μm)
low carbon steel	25	150
T22 (Fe-2.25%Cr)	20	80
T23 (Fe-2.25%Cr-1.6%W)	20	50

er/matrix interface. In this study, the effect of Cr, Mo and W as alloying elements were studied. These elements seemed to occupy the vacant sites in Al_5Fe_2 to suppress the growth rate of Al_5Fe_2 , and thereby increase the growth rate of AlFe.

4. Conclusions

The hot dip aluminizing of low carbon, T22, and T23 steels was carried out, and the microstructures were studied. The topcoat inevitably consisted primarily of Al incorporated with 0.3-0.6 %Fe. The alloy layer consisted primarily of Al_5Fe_2 in case of the low carbon steel, ($\text{Al}_5\text{Fe}_2+\text{AlFe}$) in case of the T22 steel, and AlFe in case of the T23 steel. In comparison with the low carbon steel, the thickness of the topcoat and the alloy layer was reduced, and the reaction front of the alloy layer became smooth, due to the presence Cr, Mo, and W in the substrate.

Acknowledgments

This work was supported by the Human Resource Development Project of the Korea Institute of Energy Technology Evaluation and Planning (KETEP) grant funded by the Korea government Ministry of Knowledge Economy (No. 20114010203020).

References

1. M. B. Moon, *Corros. Sci. Tech.*, **42**, 37 (2012).
2. A. Bahadur and O. N. Mohanty, *Mater. Trans. JIM*, **11**, 1053 (1991).
3. K. Bouché, F. Barbier, and A. Coulet, *Mater. Sci. Eng.*, **167**, A249 (1998).
4. S. Kobayashi and T. Yakou, *Mater. Sci. Eng.*, **44**, A338 (2002).
5. G. H. Awan and F. U. Hasan, *Mater. Sci. Eng.*, **A 157**, 472 (2008).
6. X. Si, B. Lu and Z. Wang, *J. Mater. Sci. Technol.*, **25**, 433 (2009).
7. D. Wang, *Appl. Surf. Sci.*, **254**, 3026 (2008).
8. W. J. Cheng and C. J. Wang, *Surf. Coat. Technol.*, **204**, 824 (2009).
9. J. Prohászka, J. Dobránszky, and P. J. Szabó, *X-ray*

- Spectrom.*, **28**, 233 (1999).
10. Y. Y. Chang, C. C. Tsaur, and J. C. Rock, *Surf. Coat. Technol.*, **200**, 6588 (2006).
 11. W. J. Cheng, Y. Y. Chang, and C. J. Wang, *Surf. Coat. Technol.*, **203**, 401 (2008).
 12. H. Glasbrenner, E. Nold, and Z. Voss, *J. Nucl. Mater.*, **39**, 249 (1997).
 13. J. M. Lee, S. B. Kang, T. Sato, H. Tezuka, and A. Kamio, *Mater. Sci. Eng., A* **257**, 362 (2003).